STUDY OF MICROCHANNEL HEAT SINK PERFORMANCE WITH EXPANDED MICROCHANNELS AND NANOFLUIDS

Mushtaq Ismael Hasan
Mechanical Engineering Department, College of Engineering, Thi-Qar University
mushtaq76h@ gmail.com
Received on 23 March 2016 Accepted on 20 June 2016

ABSTRACT:

In this paper a microchannel heat sink with expanded microchannels and nanofluids is numerically investigated. The object of this paper is to study and improve the cooling performance of microchannel heat sink. Both the geometrical parameters and working fluids were studied and a comparison was made between them. Expanded microchannels (sudden expanded and diverging) were used instead of straight microchannels, also micro pin fins with square and triangular shapes were used for heat transfer enhancement. Sudden expanded microchannels were studied with different expansion ratios and expansion lengths. Three types of nanofluids (Cu-water, Al_2O_3-water and Diamond-water) with volume concentration (1 – 5) % were studied as working fluids and their effects on overall performance of heat sink were compared with pure water. The results obtained shows that the overall performance of microchannel heat sink increased with increasing the expansion ratio or decreasing the expansion length. For the same expansion ratio the sudden expanded microchannels gives higher modification compared with diverging microchannels. Also using of nanofluids lead to enhance the heat transfer and the improvement got by geometric parameters such as using of expanded microchannels or fins is much larger than that obtained by using nanofluids for the same heat sink.

Key words: Sudden expansion microchannel; Microchannel heat sink; numerical investigation; diverging microchannel; Nanofluid.

Nomenclature:

Symbol	Description	SI Unit	Symbol	Description	SI Unit
A	Cross-sectional area	m^2	w	Fluid z-component velocity	m/s
c	Nanofluid concentration	%	W	Channel width	m
C_p	Specific heat	J/(kg K)	x	Axial coordinate	m
D_h	Hydraulic diameter	m	y	Vertical coordinate	m
H	Channel height	m	z	Horizontal coordinate	m
k	Thermal conductivity	W/m K	ρ	Density	kg/m^3
L	Channel length	m	μ	Dynamic Viscosity	m^2/s
m	Mass flow rate	kg/s	v_{in}	Average inlet velocity	m/s
q	Heat transfer rate	W	Abbreviations		
T	Temperature	K	nf	Nanofluid	

u	Fluid x-component velocity	m/s	*HS*	Heat sink
v	Fluid y-component velocity	m/s	*CH*	Channel

1-INTRODUCTION:

The rapid development in manufacturing of the micro devices enabled the usage of devices in microns size, such as, micro heat sink, micro biochips, micro reactors, micro motor, micro valve and micro fuel cells which are all called microfluidic devices [1]. These devices used in many applications such as micro-electronics, micro scale sensing and measurement, spacecraft thermal control, micro-electro-mechanical-systems (MEMS), and medical [2 &3]. Most of these applications include fluid flow in microchannels with dimensions in microns where the wall thickness is large and comparable to the channels dimensions. Therefore the heat transfer process cannot be simulated by the typical methods used in conventional channels. Since the heat transfer process in microchannels is a conjugated where the heat is transferred by conduction in the walls as well as in the fluids. So the energy equation must be solved in both the solid walls and fluids.

It is very essential to understand the flow phenomenon in microchannels with geometry change cases, such as sudden contractions, expansions in the design and analysis of microfluidic systems due to its direct effect on the hydrodynamics and thermal performance of these systems. Thus, a systematic investigation covering these different microchannel configurations will help to understand the flow physics. Also, the study will give vital knowledge which may be applied in the design and analysis of microfluidic systems.

One of the methods for enhancing heat transfer is the application of additives to the working fluid. The basic idea is to enhance heat transfer process by changing the fluid thermo physical properties as in nanofluid where the solid nanoparticles added to the base fluid to increase its thermal conductivity. Nanofluid composed of a base fluid such as water and nano metallic or non-metallic particles. The using a nanofluids as a heat transfer medium received much interest in recent time due to its potential advantages such as higher thermal conductivity than the pure fluids, excellent stability and small increase in pressure drop.

There are many researchers in literature studied the microchannels with different configurations and working fluids. Oliveira (2003) [4] performed a 2D planar expansion of the 1:3 expansion ratio simulations to investigate the flow field for a range of Reynolds number ranging from 0 to 100, and showed that the flow becomes asymmetric above a critical Reynolds number. Later, Revuelta (2005) [5] also presented a numerical investigation of an incompressible viscous jet through a channel with a large expansion ratio. He indicated that the critical Reynolds number depends significantly on the expansion ratio. However, the simulation results presented above only considered the two-dimensional geometry. Yu et al. (2006) [6] performed an experimental study to determine the loss coefficient due to abrupt expansion and contraction in minichannels with diameters ranging from 330 to 580 μm over a Re range of 733 to 7941. They reported that loss coefficients through an expansion were invariant with Re for laminar flow. And through a contraction decreased with increasing Re in the laminar region and remained nearly constant in the turbulent region. Chalfi (2007) [7] performed an experimental study on pressure drop caused by expansion/contraction in capillaries under low flow condition. The water flowed in two tested capillaries that had diameters of 0.84 mm and 1.6 mm. The Reynolds number covered a range of 160 to 539. He reported the minor loss coefficients for sudden contraction were nearly constant at 0.4 over the range of Re, while the minor loss coefficients for sudden expansion slightly increased with Re. Tsai et al. (2007) [8] indicated that the 2D simulation method could only be applied to predict the flow behavior in sudden expansion microchannels with high aspect ratios. In addition, they numerically examined the flow of Newtonian fluids through micro-fabricated planar expansions and demonstrated that even though the microfluidic device may have a planar geometry, the flow becomes locally 3D near the expansion region. Mushtaq et al (2009) [9] investigated numerically the effect of microchannels geometry (the size and shape of channels) on the performance of counter flow microchannel heat exchanger and used liquid water as a cooling fluid. They found that with decreasing the size of channels both the effectiveness of heat exchanger and pressure drop were increased. Also they found that the circle is the best shape for the channels of this type of heat exchangers since it gives higher overall performance. Mushtaq et al (2012)[10] numerically studied the performance of a counter flow microchannel heat exchanger with a nanofluid as a cooling medium. Two types of nanofluids were used Cu-Water and Al_2O_3-Water. They found that thermal performance of CFMCHE increased with using the nanofluids as cooling medium with no extra increase in pressure drop due to the ultra fine solid particles and low volume fraction concentrations. The nanofluids volume fractions were in the range 1 to 5%. It's also found that nanofluid-cooled CFMCHE could absorb more heat than water-cooled CFMCHE when the flow rate was low. A micro pin fin heat sink with different fins shape with two types of nanofluids (Diamond-water and Al_2O_3-water) is studied by Mushtaq I. Hasan (2014) [11]. He found that, using of nanofluid instead of pure fluid as a coolant lead to enhance the heat transfer performance by increasing the amount of heat dissipated but it also lead to increase the pressure drop for all fins shapes and nanofluids studied.

In this paper a numerical investigation is made to study two approaches lead to modify the performance of microchannel heat sink, which are microchannels configuration (sudden expanded, diverging channels and using micro pin fins) and using of nanofluids as a coolants. Then a comparison has been made between them.

2. PROBLEM DESCRIPTION:

A microchannel heat sink with different channels configurations is studied (straight channel, sudden expanded channels with different expansion ratio and diverging channels). A micro pin fins with two geometries (triangular and square) also used with expanded channels.

Fig. 1 show the schematics of microchannel heat sink with rectangular straight channels and fig. 2 show the top view of all configurations used for channels (straight, sudden expansion, diverging, and sudden expansion with triangular and square pin fins) where channels height is constant and the same for all configurations.

The dimensions of microchannel heat sink are, length (L_{HS}) is 10 mm, height (H_{HS}) is 150 µm, the width (W_{HS}) is 2.1 mm. For channels, wall thickness (t) is 100 µm, height (H_{CH}) is 100 µm, width at channels inlet (W_{chi}) is 100 µm and width at channels exit (W_{che}) is 100 µm for straight channels and variable according to the expansion ratio for expanded and diverging channels. To concentrate the study on the channels configuration, the comparison is made between different channels configurations with same heat sink volume, and the number of channels in same heat sink dimensions is different from case to case according to the configuration studied. Table 1 shows the number of channels in heat sink corresponding to each configuration. The same boundary conditions were used for all channels configurations. Pure water is used as a working fluid with properties calculated according to the average temperature in addition to three types of nanofluids (Cu-water, Al_2O_3-water and Diamond-water).

3. MATHEMATICAL MODEL:

3.1. Governing equations:

For steady state, 3D, incompressible flow the following equations are solved which are continuity, momentum and energy equations [11] and [12]:

$$\nabla V = 0 \tag{1}$$

$$\rho (V \nabla V) = -\nabla P + \mu \ (\nabla^2 V) \tag{2}$$

$$\rho C_p (V \nabla T) = k \nabla^2 T \tag{3}$$

For solid wall:

$$k_s \nabla^2 T_s = 0 \tag{4}$$

The boundary conditions used to complete the model are:

At the channel inlet the finite values of velocity and temperature were used

$T = T_{in}$, $w = v_{in}$, $u = v = 0$

At the channel outlet the flow assumed to be fully developed:

$$\frac{\partial w}{\partial x} = v = u = 0 \quad , \quad \frac{\partial T}{\partial x} = 0$$

At the lower surface of the channel a constant heat flux boundary condition is used.

The other outer surfaces of the model (right, left and top walls) are assumed adiabatic walls:

$$\frac{\partial T}{\partial z} = \frac{\partial T}{\partial x} = \frac{\partial T}{\partial y} = 0$$

All the inside surfaces that separates the solid wall and the fluid regions are used as a coupled wall with conjugate heat transfer:

$$-k \frac{\partial T}{\partial y} = -k_s \frac{\partial T_s}{\partial y}$$

Solving of above system of equations the give the distribution of the velocity, pressure and temperature. From these values the parameters to be studied such as heat transfer rate and pressure drop can be calculated from the following equations.

Heat transfer rate for one channel is:

$$Q = m\, c_p\, (T_{fe} - T_{fi}) \tag{5}$$

The total heat transfer rate for heat sink is:

$$Q_T = Q * N_{ch} \tag{6}$$

Where N_{ch} is the number of microchannels in heat sink according to the configuration used.

Pressure drop across the channel can be calculated from:

$$\Delta P = P_{in} - P_e \tag{7}$$

Where P_{in} and P_e are the total pressures in the inlet and outlet of the channels respectively.

The total pressure drop across heat sink is:

$$\Delta P_T = \Delta P * N_{ch} \tag{8}$$

And the pumping power required to circulate the fluid in the heat sink is:

$$PP = \Delta P_T * V \tag{9}$$

The factor used to calculate the overall performance of heat sink is Overall performance index (OPI) which defined as the ratio of heat transfer rate to the pumping power required which takes into account both the hydrodynamics and thermal performance of heat sink [9, 13].

$$OPI = \frac{q(W)}{PP(W)} \quad (10)$$

Reynolds number is:

$$\mathrm{Re} = \frac{\rho\, u_i D_h}{\mu} \quad (11)$$

Where D_h is the hydraulic diameter:

$$D_h = \frac{2\,(H_{ch}\, W_{ch})}{H_{ch} + W_{ch}} \quad (12)$$

Width of heat sink equal to:

$$W_{HS} = W_{ch} * N_{ch} + W_w\,(N_{ch} + 1) \quad (13)$$

For sudden expanded and diverging microchannels expansion ratio is:

$$ER = \frac{W_{che}}{W_{chi}} \quad (14)$$

And heat sink width becomes:

$$W_{HS} = W_{chi} * ER * N_{ch} + W_w\,(N_{ch} + 1) \quad (15)$$

Expansion length ratio is the ratio of length at which sudden expansion began to the total length of channel:

$$ELR = \frac{L_{ch1}}{L_{ch}} \quad (16)$$

Where L_{ch1} is the length after which the channel expanded suddenly.

4. PROPERTIES OF NANOFLUID:

The thermo physical properties of the nanofluids are depend on the properties of the base fluid, the properties of suspended solid particles, volume fraction of the solid particles in the suspension and shape of particles. Properties of nanofluids can be calculated using the following equations [14, 15]:

Thermal conductivity:

$$k_{nf} = k_f \left[\frac{k_p + (SH-1)k_f - (SH-1)c(k_f - k_p)}{k_p + (SH-1)k_f + c(k_f - k_p)}\right] \quad (17)$$

Viscosity:

$$\mu_{nf} = \mu_f (1 + 2.5c) \quad (18)$$

Density:

$$\rho_{nf} = c\rho_p + (1-c)\rho_f \tag{19}$$

Specific heat:

$$Cp_{nf} = cCp_p + (1-c)Cp_f \tag{20}$$

Where: SH is solid particle shape factor.

$$SH = \frac{3}{\psi} \tag{21}$$

ψ is sphericity defined as the ratio of the surface area of a sphere with a volume equal to that of the particle to the surface area of the particle. For spherical particles SH = 3.
Where subscripts f, nf, p refer to the base fluid, nanofluid and solid particles respectively.

In this paper three nanofluids were used. Water is the base fluid used for all of them and the solid particles are cupper (Cu) for the first nanofluid, Aluminum oxide (AL_2O_3) for the second and Diamond for third. All the three nanofluids used with volume fractions (1 %, 2 %, 3 %, 4%, 5 %).

The properties used of Cu nanoparticles are density is 3930 (kg / m^3), thermal conductivity is 386 (W / m.K) , specific heat is 383.1 (J / kg.K), and for AL2O3 are density is 3600 (kg / m^3), thermal conductivity is 36(W / m.K), specific heat is 765 (J / kg.K), Also for Diamond are density is 3510 (kg / m^3), thermal conductivity is 1000 (W / m.K), specific heat is 497.25(J / kg.K).

5. NUMERICAL SOLUTION:

The above system of equations and boundary conditions are numerically solved using finite volume method. The flow is developing and the heat transfer is conjugated process therefore the 3D continuity and 3D Navier-Stokes equations are solved in flow region while the 3D energy equation is solved in both the fluid and solid wall regions.

SIMPLE algorithm is used to solve the problem of velocity-pressure coupling and the upwind scheme is used to discritize the equations [16, 17].

A mesh has been chosen in accepted size and the mesh refinement study has been made to find out the effect of mesh size on the accuracy of numerical solution. Table 2 shows that, the solution becomes independent of grid size and from third mesh further increase in the grids will not have a significant effect on the solution and results of such arrangement are acceptable. Therefore and for maximum accuracy the fourth mesh size is used for all calculations.

The convergence criteria used to control the numerical solution for both momentum and energy equations are 10^{-6}.

6. RESULTS AND DISCUSSION:

6.1. Validation:

To check the validity of the built numerical model, verification was made by solving the experimental model presented in Weilin Q. [18] and the results were compared. The experimental model presented in Weilin Q. [18] is a microchannel heat sink consists of rectangular microchannels with hydraulic diameter 348.9 μm, channel height 713 μm, channel width 231 μm and length 4.48 cm. Temperature was measured in four points along the channel bottom wall, and experiment was made with inlet velocity of 1 m/s, inlet temperature of 288 K and thermal boundary condition is a constant heat flux of 100 W/cm2 subjected on the bottom wall of the substrate

Fig. 3 shows the comparison between results of present numerical model and the experimental data of [18] for temperature distribution along the bottom wall of the channel. From this figure it can be seen that, the agreement between numerical and experimental results is acceptable since the maximum error is 1.41% which may be due to the end effect. Therefore the present numerical model is reliable and can be effectively.

6.2. Results:

Fig. 4 shows the contour of velocity for both straight and sudden expanded channels (ER = 2.333) at longitudinal central (x-z) plan (y = 0.00005 m) for Re=100 with pure water. From this figure it can be seen that, for straight channels the velocity profile follow the parabolic distribution also it can be seen the entrance region in the beginning of straight channels since the flow is developing and the velocity increased from the walls toward center of channel. While in expanded channel the flow follow the same behavior in the region before the expansion and then started to develop again after expansion region due to mixing occurred also there are vortices created in the coroners.

Fig.5 represent the temperature contour for both straight and sudden expanded channels (ER = 2.333) at longitudinal central (x-z) plan (y = 0.00005 m) for Re=100 with pure water. From this figure it can be observed that, the temperature increased along flow direction due to heat transfer from lower wall with constant heat flux. The increase in temperature continue along the straight channel while for expanded channel the flow is expanded after the expansion region and start to developing again due to expansion and mixing occurred which lead for extra heat transfer since as it clear from the figure the temperature at the channel exit much higher than that for straight channel.

Fig.6 indicate the variation of total heat transfer rate with Reynolds number for straight channels and sudden expanded channels with different values of expansion ratio for pure water and same value of subjected heat flux. From the figure one can see that, the total amount of heat transferred by heat sink increased with increasing the expansion ratio due to increasing the heat transfer with expansion as explained in figure 5. Also all expansion ratio cases have higher heat transfer rate compared with straight microchannel. The heat transfer increased also with increasing Reynolds number due to increasing flow rate.

Fig.7 shows the variation of total pressure drop with Reynolds number for straight channels and sudden expanded channels with different values of expansion ratio for pure water. From this figure it can be seen that, the total pressure drop in case of sudden expanded channels less than that for straight channels and it decreased with increasing expansion ratio due to dispersion the fluid in larger area and reducing the effect of friction and reducing the velocity of flow in expanded channels. Also the pressure drop increased with increasing Reynolds number for all cases due to increasing the friction effects.

Fig.8 represent the variation of overall performance index with Reynolds number for straight channels and sudden expanded channels with different values of expansion ratio for pure water and same value of subjected heat flux. This parameter take into consideration both the hydrodynamics and thermal performances and give an overall evaluation for cases studied. From this figure it can be observed that, the heat sink with sudden expanded channels give higher overall performance compared with that for straight channels and the OPI increased with increasing the expansion ratio for all range of Reynolds number due increasing the heat transferred and reducing the pressure drop. The OPI decreased with increasing Reynolds number which mean that, the increment in pressure drop become larger than the increment in heat transfer.

The variation of total heat transfer with Reynolds number for both straight channels and sudden expanded channels with different values of expansion length ratio for ER = 1.5 is indicated in fig.9. This figure show that, the sudden expanded channels give higher heat transfer performance compared with straight channels as explained before and the total heat transfer increased with decreasing the expansion length ratio because as the expansion length reduced the effect of entrance region will appear and also because the increasing the heat transfer area. The total heat transfer show increasing with Reynolds number as explained before.

Fig.10 show the variation of total pressure drop with Reynolds number for both straight channels and sudden expanded channels with different values of expansion length ratio for ER = 1.5. It can be observed from this figure that, the pressure drop for heat sink with suddenly expanded microchannels less than that for one with straight microchannels due to increasing the expanded area for channels as the expansion start near to the channels inlet.

Fig. 11 represent the variation of OPI with Re for both straight channels and sudden expanded channels with different values of expansion length ratio for ER = 1.5. This figure reveal that, early starting of sudden expansion with respect to channel length lead to improve the overall performance due to enhancing heat transfer and reducing pressure drop as explained before and the final gain is increasing the OPI values since it increased with decreasing the expansion length ratio, and all cases of sudden expanded channels give higher value of OPI compared with straight channels. Also the values of OPI decreased with increasing Re as explained before.

Variation of total heat transfer rate with Reynolds number as a comparison between heat sink with straight channels, sudden expanded channels (ER = 1.5) and diverging channels (ER = 1.5) under the same boundary condition is indicated in fig. 12 to study the use of diverging channels instead of sudden expanded channels. From this figure it can be seen that, for all range of Reynolds number the sudden expanded channels give much higher heat transfer performance compared with both straight and diverging channels due to sudden expansion effects such as vortices occurred at the expansion region which lead to extra mixing for fluid. Also the heat transferred for diverging channels is higher than that for straight channels due to increasing the heat transfer area and reduction in flow velocity with direction of flow in which the fluid get extra opportunity to exchange heat and absorb extra amount of heat. As appeared and explained in previous figures the heat transfer rate increased with increasing Reynolds number.

Fig.13 show the variation of OPI with Re for heat sink with straight, sudden expanded (ER = 1.5) and diverging channels (ER = 1.5). From this figure one can observe that, also the sudden expanded channels give higher overall performance followed by diverging and straight channels due to enhancing the heat transfer efficiency and the reduction in pressure drop. Also the OPI reduced with increasing Re because the increment occurred in pressure drop become larger than the increment in heat transfer as Re increase.

In figures (14 and 15) the effect of adding micro pin fins with triangular and square shapes to the sudden expanded channels is studied. Fig.14 represent the variation of total heat transfer rate with Re for sudden expanded channels (ER = 2.333) with and without fins. From this figure can be see that, the square fin give higher heat transfer efficiency by transferring larger amount of heat compared with triangular fin and with channels without fin due to the triangular fin is more smooth in flow direction and cause less mixing in fluid while the square fin cause higher mixing and disturbance in flow which lead to enhancing heat transfer process. Also the heat transfer rate increased with increasing Re for all geometries studied. The variation of OPI with Re is represented in fig.15 which indicate that, also the square fin lead to higher overall performance compared with other configurations but the difference between channels with square and triangular fins become too small and the performance of channels with triangular fin approach that for square fin because the extra increase in pressure drop in square fin compared with triangular fin lead to decrease the OPI for square and approaching in its values for two fins. Also the OPI decreased with increasing Re for all configurations.

In figures (16 to 19) the results of using three types of nanofluids (Cu-water, AL_2O_3-water and Diamond-water) instead of pure water are presented. Fig.16 show the variation of total heat transfer rate of straight channels using Cu-water nanofluid with nanoparticles concentration. This figure reveal that, the heat transfer rate increased with increasing nanofluid concentration due to modification of the fluid thermal properties especially the thermal conductivity compared with pure water and this modification continue with adding extra amount of nanoparticles but the maximum value of concentration used here is 5 % as discussed before. Variation of total heat transfer rate in straight channels with pure water and three types of nanofluids with Re is indicated in fig17. From this figure it can be noted that, the heat transferred for straight channels with all three types of nanofluids higher than that for straight channels with pure water due to increasing the thermal conductivity of fluid. The Cu-water nanofluid give higher heat transfer performance among all others because it has higher thermal conductivity compared with other two nanofluids and pure water, and it followed by Al_2O_3 - water and Diamond – water respectfully. Also the heat transfer rate increased with increasing Re for all fluids studied.

To compare between the improvement in heat sink performance caused by geometry and using different types of fluids the fig.18 represent the comparison between different geometrical configurations studied and the straight channels with best nanofluid (Cu-water). This figure show the variation of total heat transfer rate with Re for all mentioned cases. The geometrical configurations selected are (sudden expanded channels with ER = 2.333 because it the best one compared with other sudden expansion configurations, the diverging channels, the sudden expanded channels (ER = 2.333) with two types of fins). From this figure it can be seen that, the sudden expanded channels with square fin give higher heat transfer rate followed by sudden expanded channels with triangular fin, sudden expanded channels (ER = 2.333), straight channels with Cu-water nanofluid and diverging channels respectfully. Also for all cases mentioned above the heat transfer rate increased with increasing Re.

Fig.19 show the variation of total heat transfer rate with nanofluid concentration in case of using Cu-water nanofluid as a cooling fluid with sudden expanded channels (ER = 2.333) with square fin which represent the best case among all geometrical cases studied previously. This figure indicate that, the total heat transfer rate in this case increased with increasing nanofluid concentration as a results of increasing thermal conductivity of nanofluid with increasing the amount of nanoparticles immersed in pure water.

7. Conclusions:

From the results obtained in this paper it can be concluded the following:

1-Geometrical parameters lead to higher improvement in microchannel heat sink compared with using different types of working fluids. So the researchers must pay more attention for these parameters.

2- For sudden expanded microchannels, increasing of expansion ratio and decreasing the expansion length both lead to increasing the overall performance of microchannel heat sink.

3- Sudden expansion microchannel caused larger improvement in microchannel heat sink compared with diverging microchannels.

4- Using of micro pin fins in microchannels improve the performance of microchannel heat sink and the square fins give higher improvement.

5- Using of nanofluids as cooling fluids instead of pure water lead to improve the thermal and overall performance of microchannel heat sink and the Cu-water nanofluid is the best compared with two types of nanofluids studied (Al_2O_3-water and Diamond-water).

6- Combination of improvement in geometrical configurations and using of nanofluids as coolants give additional improvement in microchannel heat sink.

7-REFERENCES:

[1] Barbaros, C., Almila, G. Y., Sadik, K., fluid flow in microtubes with axial conduction including rarefaction and viscous dissipation, Int. J. of Heat and Mass Transfer, 34, pp. 535-544, 2008.

[2] Poh, S. L., Suresh, V. G., Dong L., Investigation of heat transfer in rectangular microchannels, Int. Journal of heat and Mass Transfer, 48 (9), pp. 1688 - 1704, 2005.

[3] Jun, Y., Mayur, K. P., Yufeng, Y., Peter, J. M., Numerical simulation of heat transfer in rectangular microchannel, European Conference on Computational Fluid Dynamics ECCOMAS CFD, TU Delft, Netherlands, 2006.

[4] Oliveira, P.J., Asymmetric flows of viscoelastic fluids in symmetric planar expansion geometries, J. Non-Newt Fluid Mech., 114, pp.33–63, 2003.

[5] Revuelta, A., on the two-dimensional flow in a sudden expansion with large expansion ratios, Phys Fluids 17, 2005.

[6] Yu, J., Li, Z., Ma, C.F., Experimental Study of Pressure Loss Due to Abrupt Expansion and Contraction in Mini-Channels, MIC-19, International Heat Transfer Conference, 13, 2006.

[7] Chalfi, T., Pressure Loss Associated with Flow Area Change in Micro- Channels, MS Thesis, Dept. of Mechanical Engineering, Georgia Institute of Technology, 2007.

[8] Tsai, CH., Chen, H. T., Wang, Y. N., Lin, CH., Fu, L.M., Capabilities and limitations of 2-dimensional and 3-dimensional numerical methods in modeling the fluid flow in sudden expansion microchannels, Microfluid Nanofluid 3, pp.13–18, 2007.

[9] Mushtaq, I. H., Abdul Muhsin, A. R., Yaghoubi, M., Homayony, H., Influence of channel geometry on the performance of counter flow microchannel heat exchanger, Int. J. of thermal sciences, Vol. 48, 1607–1618, 2009.

[10] Mushtaq I. H., Abdul Muhsin, A. R., Yaghoubi, M., Investigation of a counter flow microchannel heat exchanger performance with using nanofluid as a coolant, Journal of Electronics Cooling and Thermal Control, Scientific Research, 2, pp. 35-43, 2012.

[11] Mushtaq I. H., Investigation of Flow and Heat transfer Characteristics in Micro Pin Fin Heat Sink with Nanofluid, J. of Applied Thermal Engineering, Vol. 63, 598-607, 2014.

[12] Incropera, F. P., Dewitt, D., P., Fundamentals of heat and mass transfer, 4th Edition, Jhon Wiley and sons, 1996.

[13] Mushtaq, I. H., Numerical investigation of counter flow microchannel heat exchanger with MEPCM suspension, J. of Applied Thermal Engineering, 31, pp. 1068-1075, 2011.

[14] Tsung, H. T., Reiyu, C., Performance analysis of nanofluid-cooled microchannel heat sinks, Int. Journal of Heat and Fluid Flow 28, 1013- 1026, 2007.

[15] Jaeseon, L., Issam, M., Assessment of the effectiveness of nanofluids for single - phase and two - phase heat transfer in micro-channels, Int. Journal of Heat and Mass Transfer 50, 452-463, 2007.

[16] Versteeg, H. K., Malasekera, W., An introduction to computational fluid dynamic (The finite volume method), Addison Wesley Longman Limited, 1995.

[17] Patankar, S.V., Numerical heat transfer and fluid flow, Hemisphere Publishing Corporation, 1980.

[18] Weilin Q., and Issam, M., Thermal design methodology for high heat flux single phase and two phase microchannel heat sinks, IEEE Trans. Components and Packaging Technologies 26, pp.598-609, 2003.

Table 1 number of channels according to channels configuration

Channels configuration	Number of channels
Straight channels	10
Sudden expanded channels (ER = 1.222)	9
Sudden expanded channels (ER = 1.5)	8
Sudden expanded channels (ER = 1.857)	7
Sudden expanded channels (ER = 2.333)	6
Diverging channels (ER = 1.5)	8

Table 2 Grid independence study

Mesh size	Outlet temperature (K)	Pressure drop (Pa)
mesh1 (8,8,80) in (x,y,z) directions	333.6	97888
mesh2 (9,9,90) in (x,y,z) directions	333.48	9911
mesh3 (10,10,100) in (x,y,z) directions	333.39	10002
mesh4 (12,12,100) in (x,y,z) directions	333.3	10092

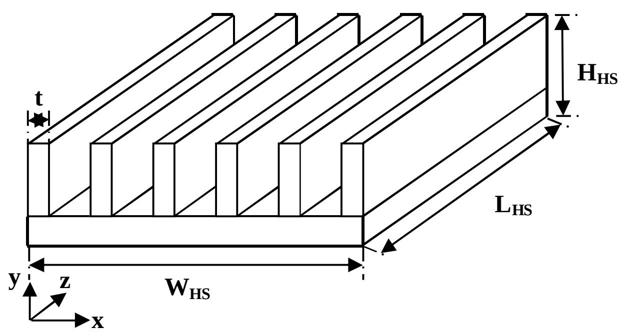

Fig. 1 schematic of microchannel heat sink with straight rectangular microchannels

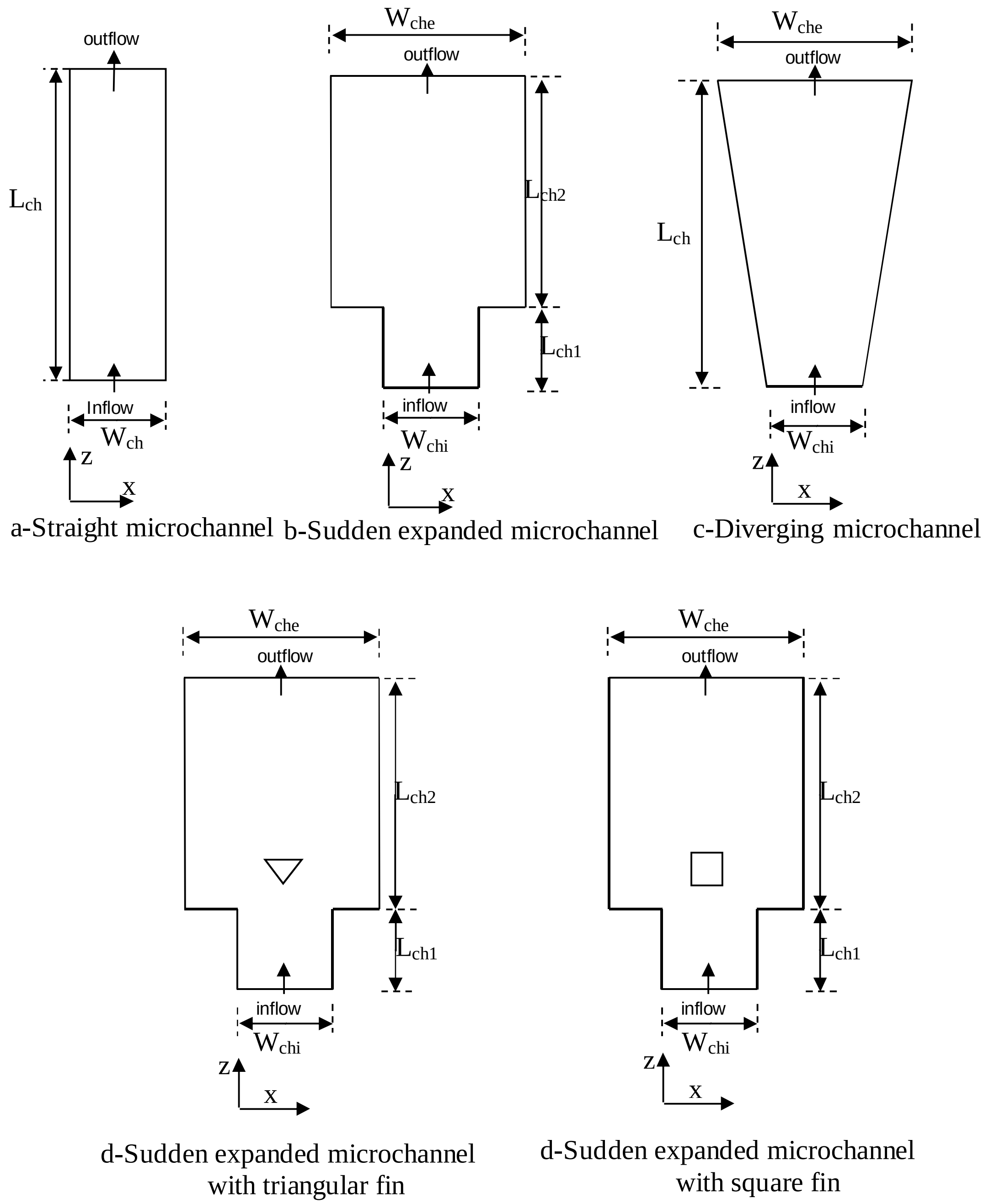

Fig.2 schematics of studied channels configurations (top view)

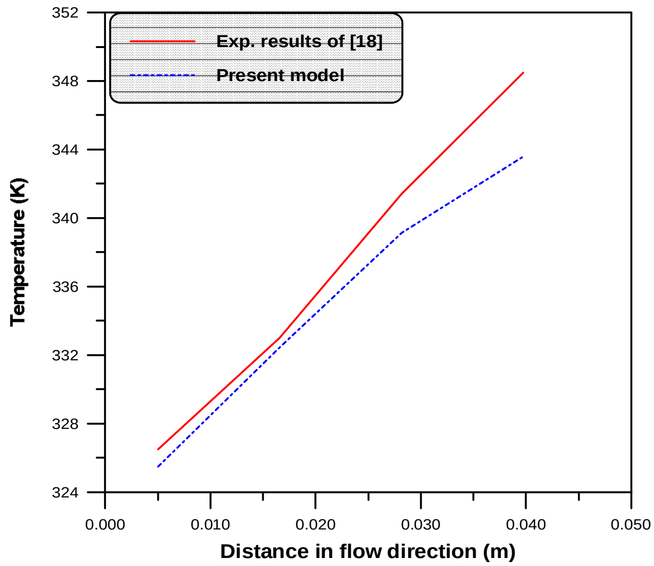

Fig. 3 variation of wall temperature in flow direction as a comparison between present model and [18]

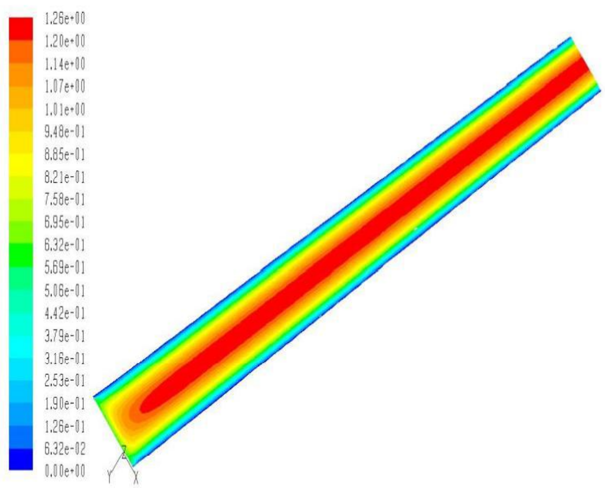

a-Straight microchannel

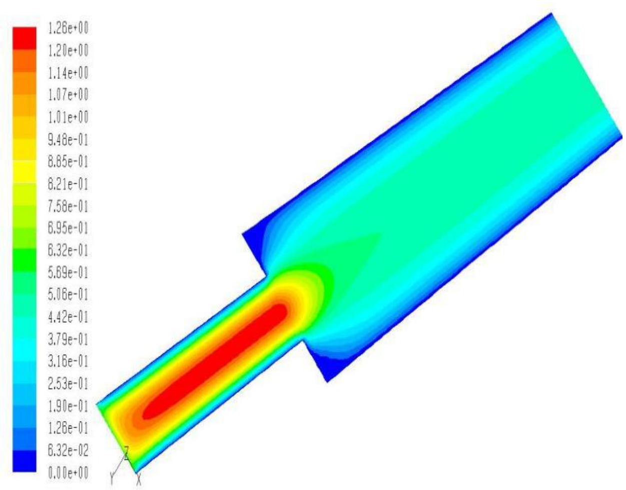

a-Sudden expanded microchannel

Fig. 4 velocity contour at longitudinal central plan (y=0.00005m), Re=100

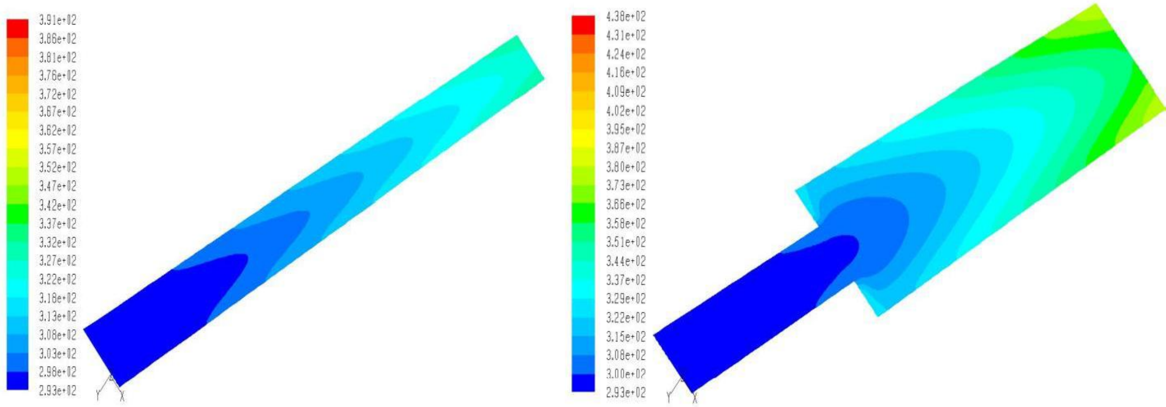

a-Straight

b-Sudden expanded microchannel

Fig. 5 Temperature contour at longitudinal central plan (y=0.00005m), Re=100

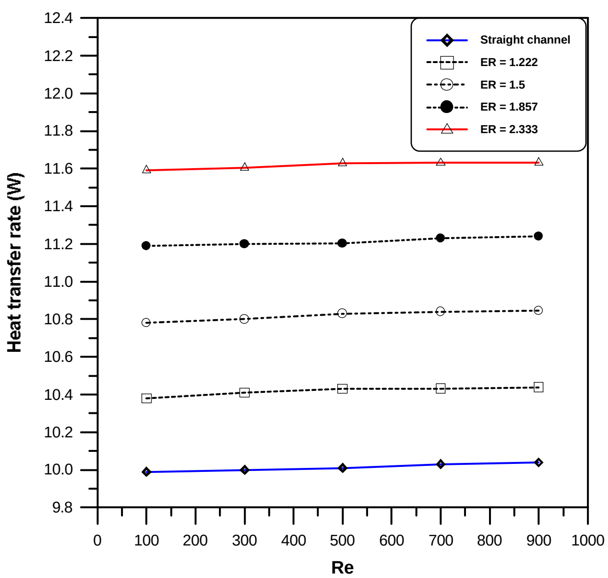

Fig. 6 variation of total heat transfer rate with Re for straight and sudden expanded channels

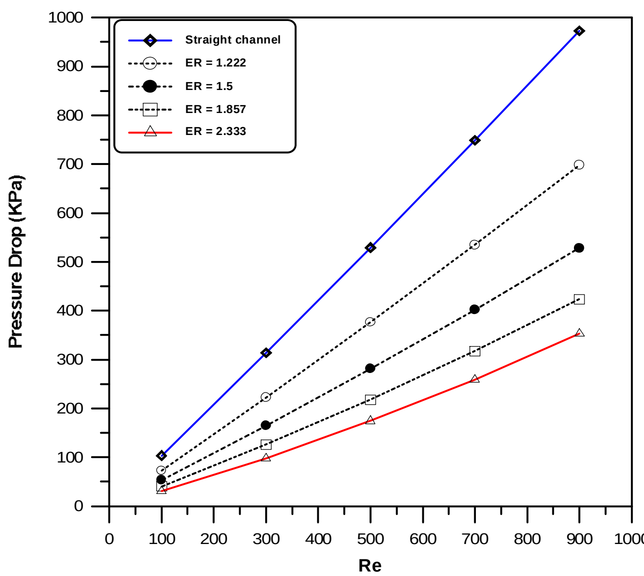

Fig. 7 variation of total pressure drop with Re for straight and sudden

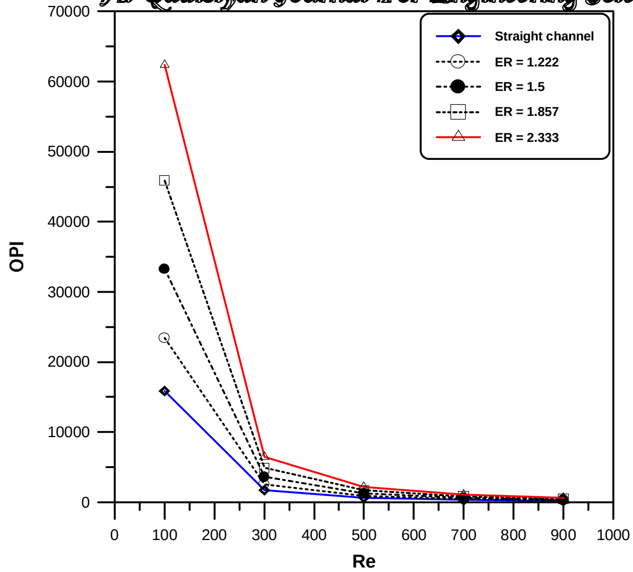

Fig. 8 variation of overall performance index with Re for straight and expanded channels

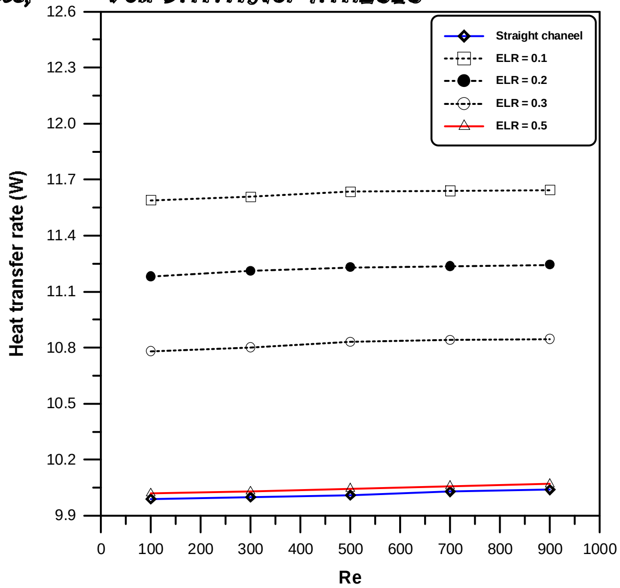

Fig. 9 variation of total heat transfer rate with Re for straight and sudden expanded channels with different expansion length ratio

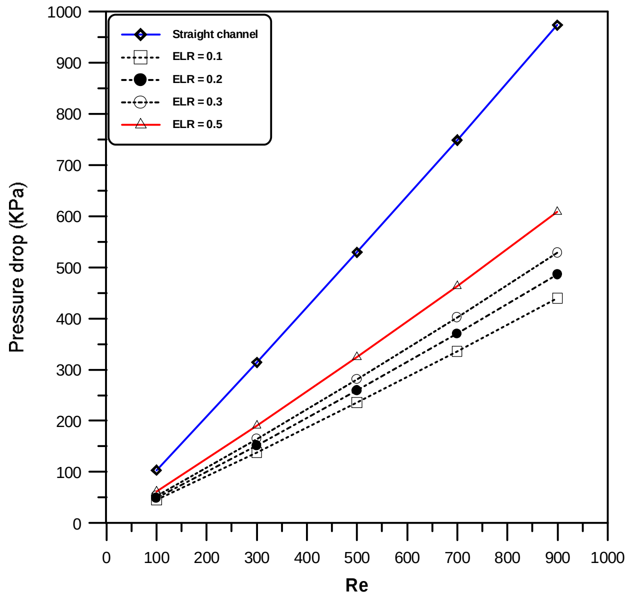

Fig. 10 variation of total pressure drop with Re for straight and sudden expanded channels with different expansion length ratio

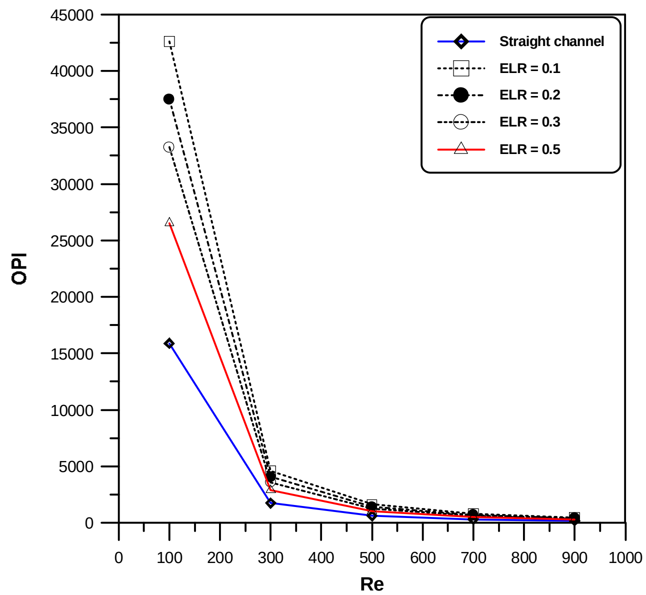

Fig. 11 variation of overall performance index with Re for straight and sudden expanded channels with different expansion length ratio

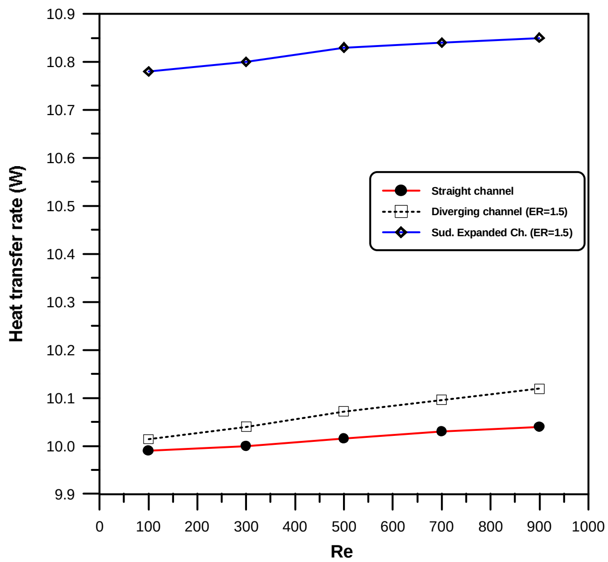

Fig. 12 variation of total heat transfer rate with Re for straight, diverged and sudden expanded channels

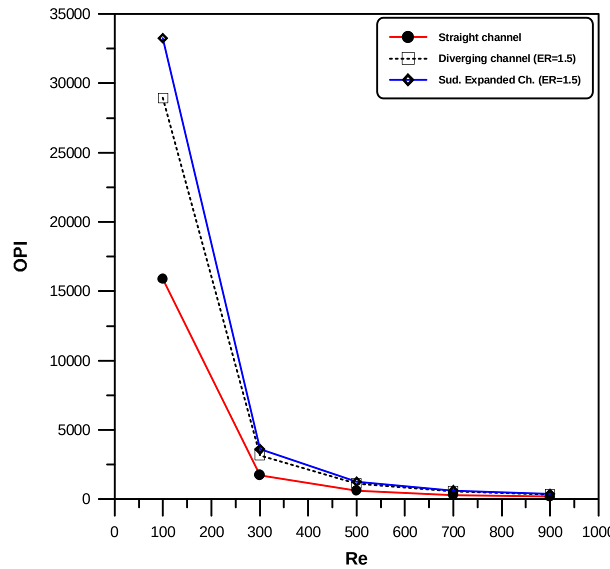

Fig. 13 variation of OPI with Re for straight, diverged and sudden expanded channels

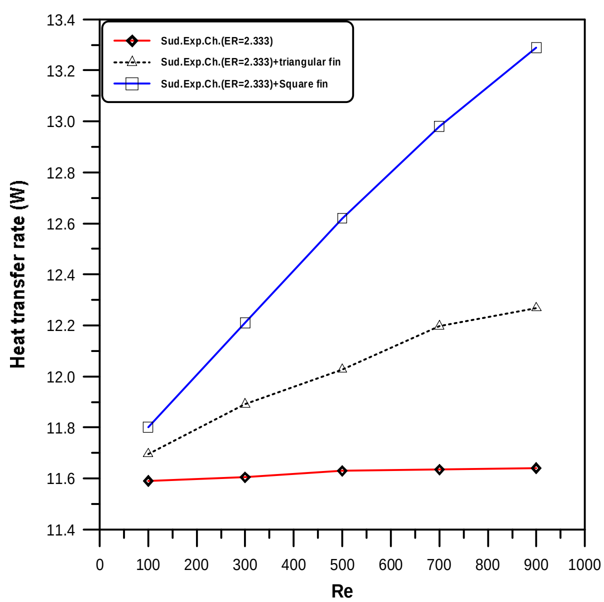

Fig. 14 variation of total heat transfer rate with Re for sudden expanded channels with triangular and square fins

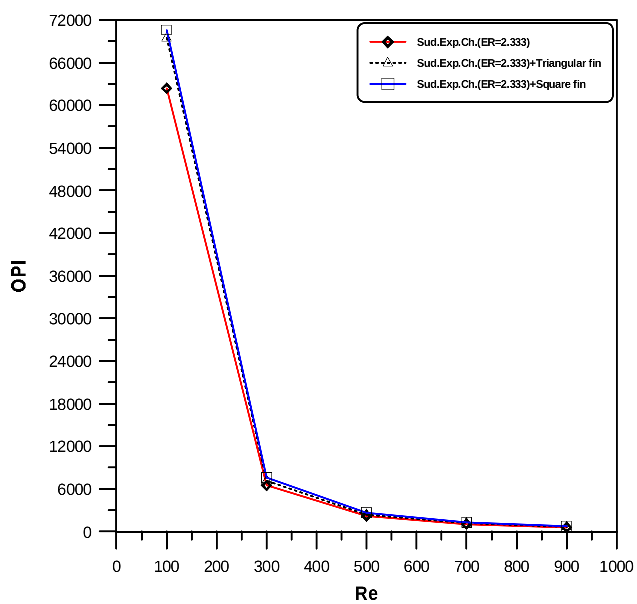

Fig. 15 variation of OPI with Re for sudden expanded channels with triangular and square fins

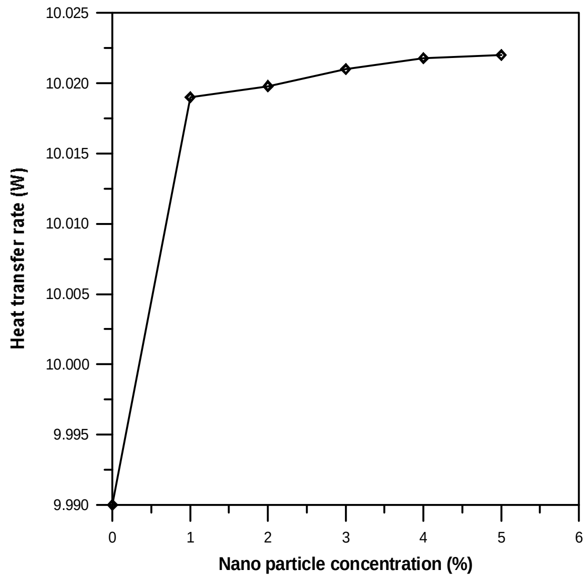

Fig. 16 variation of total heat transfer rate with c for straight channel with Cu-water nanofluid

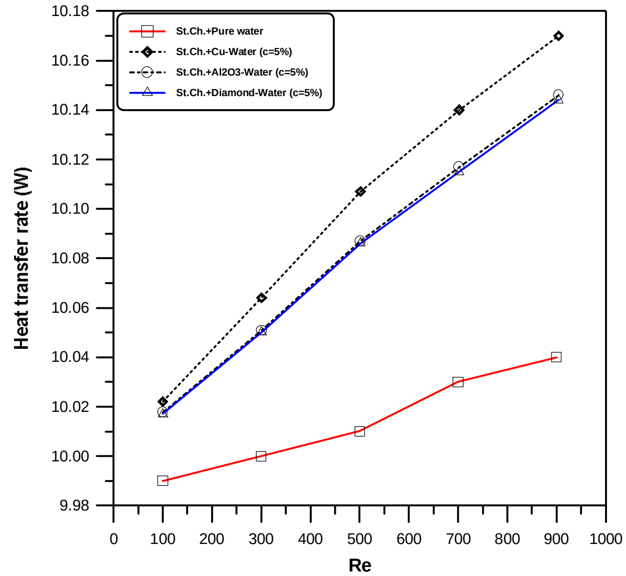

Fig. 17 variation of total heat transfer rate with Re for straight channels with pure water and three types of nanofluids

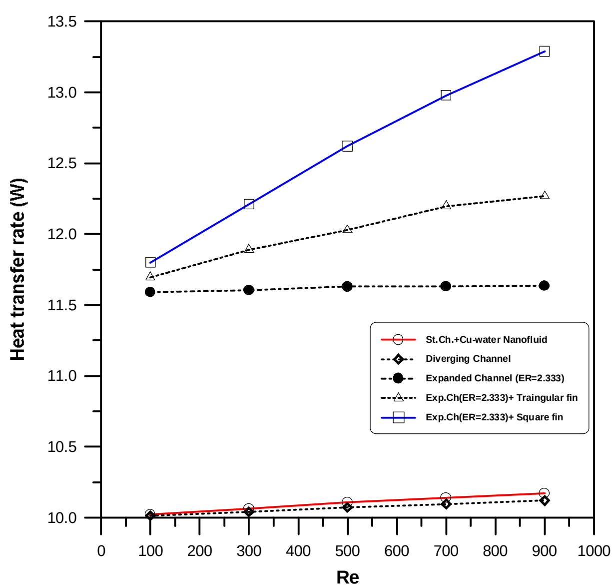

Fig. 18 variation of total heat transfer rate with Re for different cases studied

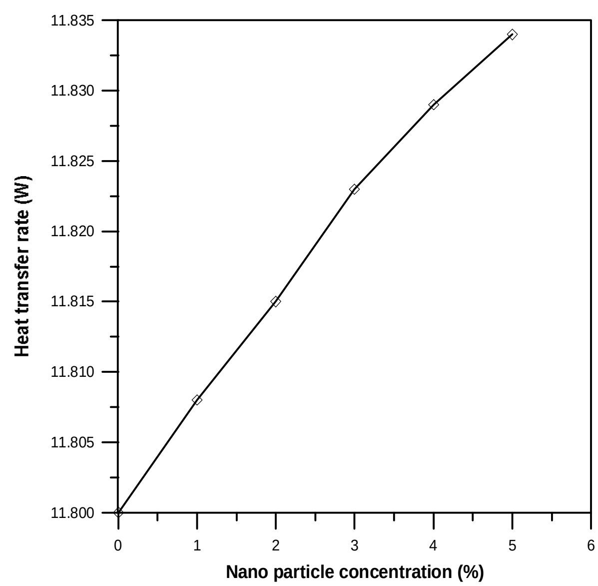

Fig. 19 variation of total heat transfer rate with c for sudden expanded channel with square fin and Cu-water nanofluid